Properties of Zr hypernuclei in deformed Skyrme Hartree-Fock approach*

WEI Ning(魏宁)[1)] ZHOU Xian-Rong(周先荣)[2)] CHEN Fang-Qi(陈芳祁)

(Department of Physics and Institute of Theoretical Physics and Astrophysics, Xiamen University, Xiamen 361005, China)

Abstract Properties of the even-N Zr isotopes and their corresponding single-Λ and double-Λ hypernuclei are studied in the deformed Skyrme-Hartree-Fock approach. Binding energy, the two-neutron separation energies, radii are studied from beta-stable zone to the neutron drip line in this paper. The neutron drip line nuclei predicted with SLy4 and SkI4 interactions are ^{122}Zr and ^{138}Zr, respectively. The neutron drip line of single-Λ and double-Λ hypernuclei are $^{139}_{\Lambda}$Zr and $^{142}_{2\Lambda}$Zr with SkI4 interaction, respectively. The predicted hyperon drip line hypernuclei with ^{80}Zr and ^{138}Zr cores are $^{100}_{20\Lambda}$Zr and $^{188}_{50\Lambda}$Zr, respectively.

Key words Deformed Skyrme-Hartree-Fock, neutron drip line, two-neutron separation energy, neutron halo

PACS 21.80.+a, 21.10.Dr, 21.10.Gv

1 Introduction

The developments of radioactive nuclear beams are changing the field of nuclear research from the beta-stable region towards the drip line. Exotic phenomena such as neutron skin and neutron halo have been found. The discovery of neutron halo nucleus, ^{11}Li in 1985[1], has brought much excitement to the atomic and nuclear physics communities. It can be described briefly as a very loosely bound particle tunneling into the space surrounding a potential well in a process represented by an extended dilute wave-function tail[2]. In Ref. [3], the neutron halo was reproduced in a self-consistent way, without further modification, using the scattering of cooper pairs to the $2s1/2$ level in the continuum, excellent agreement with recent experimental data is observed. Moreover,a giant halo which composed by as many as six neutrons in Zr was predicted by this model[4]. However, the existence of halo structure in Zr is model dependent in the Hartree-Fock-Bogoliubov calculation[5]. The Skyrme parameter SkI4 and Sly4 were used in the calculation, and only the former predicted a halo in Zr isotopes with $A>122$.

The hyperon can be free from the Pauli blocking by nucleons, which made it possible to probe deep into the nucleus, and thus become an ideal tool to study the properties of the nuclei. Besides, the hyperon can provide attractive $\Lambda-N$ interaction which would be helpful in the formation of the neutron halo. Therefore the properties of neutron halos and giant halos in hypernuclei would be very interesting. In this paper, the properties of Zr isotopes and its corresponding hypernuclei were studied in the deformed Skyrme-Hartree-Fock approach[6].

This paper is organized as follows. In sec. 2 we briefly describe the theoretical framework. In sec. 3 the calculation result are presented . Finally, a discussion of the results and our conclusions are contained in Sec. 4.

2 Theoretical framework

Our model is based on the deformed self-consistent Skyrme-Hartree-Fock methods[6] solved in

Received 3 September 2008

* Supported by National Natural Science Foundation of China (10605018) and program for New Century Excellent Talents in University(NCET-07-0730)

1) E-mail: nwei@xmu.edu.cn

2) E-mail: xrzhou@xmu.edu.cn

the coordinate space with axially symmetric shape[7]. More details are given in Ref. [8] and the Refs therein. The total energy of a hypernucleus in the extended Deformed Skyrme-Hartree-Fock model is expressed as

$$E = \int \mathrm{d}^3 r \varepsilon(r) \tag{1}$$

with the energy density functional

$$\varepsilon = \varepsilon_{\mathrm{N}}[\rho_{\mathrm{n}}, \rho_{\mathrm{p}}, \tau_{\mathrm{n}}, \tau_{\mathrm{p}}, J_{\mathrm{n}}, J_{\mathrm{p}}] + \varepsilon_{\Lambda}[\rho_{\mathrm{n}}, \rho_{\mathrm{p}}, \rho_{\Lambda}, \tau_{\Lambda}], \tag{2}$$

where ε_{N} is the total energy density of neutrons and protons[6, 9], and the local density ρ_{q}, kinetic density J_{q}, and spin-orbit current J_{q} read

$$\rho_{\mathrm{q}} = \sum_{i=1}^{N_{\mathrm{q}}} n_{\mathrm{q}}^i |\phi_{\mathrm{q}}^i|^2 , \tag{3}$$

$$\tau_{\mathrm{q}} = \sum_{i=1}^{N_{\mathrm{q}}} n_{\mathrm{q}}^i |\nabla \phi_{\mathrm{q}}^i|^2 , \tag{4}$$

$$J_q = \sum_{i=1}^{N_{\mathrm{q}}} n_{\mathrm{q}}^i \phi_{\mathrm{q}}^{i\,*} (\nabla \phi_{\mathrm{q}}^i \times \boldsymbol{\sigma})/i , \tag{5}$$

where ϕ_{q}^i $(i = 1, N_{\mathrm{q}})$ are the single-particle wave functions of the N_{q} occupied states for particles of kind q=n,p,Λ. The occupation probabilities n_{q}^i (for nucleons only) are calculated by taking a residual pairing interaction into account, which is taken to be a density-dependent delta-force[10],

$$V_{\mathrm{q}}(r_1, r_2) = V_{\mathrm{q}}' \left(1 - \frac{\rho_{\mathrm{N}}(r)}{\rho_0}\right) \delta(r_1 - r_2), \tag{6}$$

where $\rho_{\mathrm{N}}(r)$ is the HF density at $r = (r_1 + r_2)/2$ and $\rho_0 = 0.16\ \mathrm{fm}^{-3}$. The pairing strength is taken to be $V_{\mathrm{p}}' = -1146\ \mathrm{MeV\ fm}^3$, $V_{\mathrm{n}}' = -999\ \mathrm{MeV\ fm}^3$.

The minimization of the total energy Eq.(1) implies the SHF Schrödinger equation

$$\left[-\nabla \cdot \frac{1}{2m_{\mathrm{q}}^*(r)} \nabla + V_{\mathrm{q}}(r) - \mathrm{i} \nabla W_{\mathrm{q}}(r) \cdot (\nabla \times \boldsymbol{\sigma})\right] \phi_{\mathrm{q}}^i(r) = e_{\mathrm{q}}^i \phi_{\mathrm{q}}^i(r). \tag{7}$$

3 Results

The two-neutron separation energy is crucial to judge the neutron drip line, and expose the structure of the nucleus. It is defined as

$$S_{2\mathrm{n}}(N, Z) = E(N, Z) - E(N-2, Z), \tag{8}$$

where $E(N,Z)$ is the total energy of the nucleus with N neutrons and Z protons. The two-neutron separation energy for Zr isotopes and its corresponding hypernuclei with single-Λ and double-Λ hyperons were calculated by SHF with SkI4 interaction and Zr isotopes with SLy4 interaction as a comparison.

The binding energies of Zr isotopes from ^{80}Zr to ^{110}Zr, which the experiment can reached until now, with SLy4, SkI4 interactions and experimental data are shown in Fig. 1. The binding energies with SLy4 and SkI4 interactions were generally 2 MeV different from the experimental data. The maximal with SLy4 interaction is 4.8582 MeV while 3.9388 MeV with SkI4 interaction at ^{110}Zr. It is not possible to tell which Skyrme parameters is better for Zr isotopes from the experimental data. Then we studied the radii, two-neutron separation energies with SLy4 and SkI4 interactions, respectively. The neutron drip line nuclei predicted with SLy4 and SkI4 interactions are ^{122}Zr and ^{138}Zr, respectively, which agrees with Ref. [5].

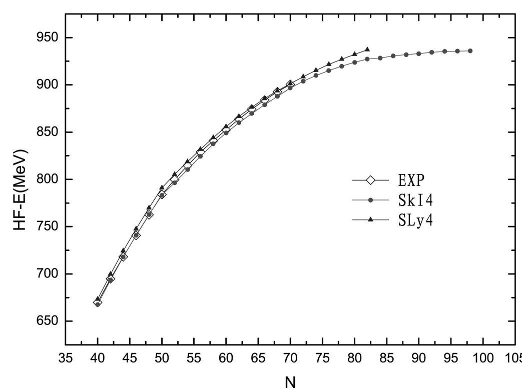

Fig. 1. Results from DSHF calculation with SLy4, SkI4 interactions and experimental data

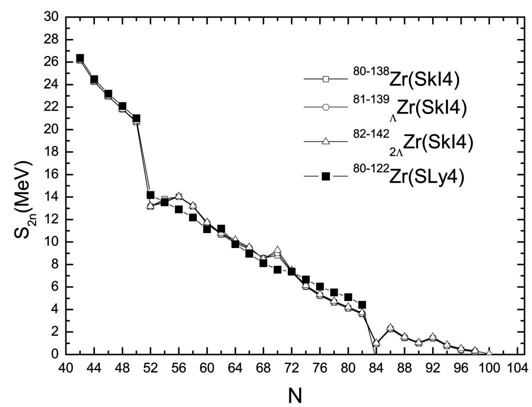

Fig. 2. The two-neutron separation energies for Zr isotopes with SLy4 and SKI4 interactions, respectively.

In Fig. 2 the neutron drip line of the corresponding hypernuclei with SkI4 are $^{139}_{\Lambda}$Zr and $^{142}_{2\Lambda}$Zr, respectively. There are two additional neutrons in the last bound hypernucleus, $^{142}_{2\Lambda}$Zr, compared to the corresponding ordinary nuclei, because of the additional attractive force provided by the Λ-N interaction. The two-neutron separation energies for the last bound nucleus with SkI4 and SLy4 interactions, are 0.2295 MeV for ^{138}Zr and 4.4229 MeV for ^{122}Zr, respectively. It decreased sharply when the mass number beyond 122, while 3.5913 MeV for ^{122}Zr, 0.9414 MeV for ^{124}Zr, 2.2443 MeV for ^{126}Zr with SkI4 interaction. Because the small two-neutron separation energies in the continuum nuclei could be a signature for the existence of neutron halo, the former force predicts a neutron halo with mass number beyond 122. We get the same results as vividly shown in Fig. 3.

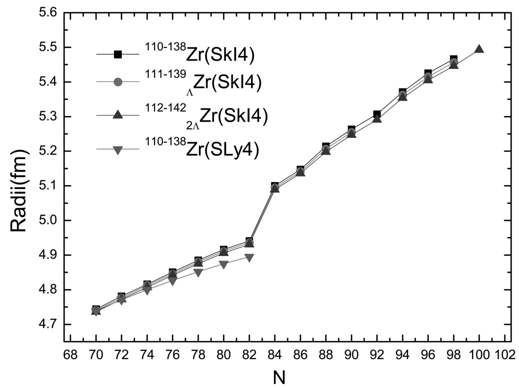

Fig. 3. Neutron radii for Zr isotopes with SLy4, SkI4 interactions and corresponding hypernuclei as a function of neutron numbers.

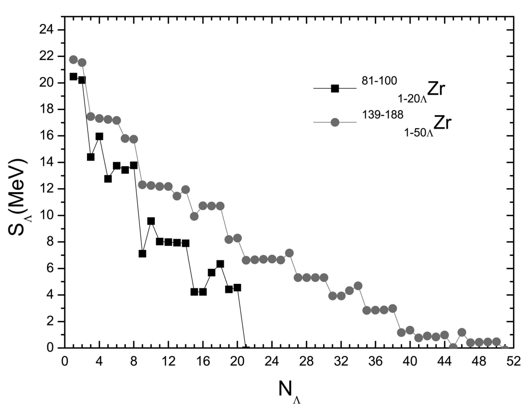

Fig. 4. The hyperon separation energy as a function of hyperon numbers. The solid circle indicate multi-Λ hypernuclei with a ^{80}Zr core and solid square with a ^{138}Zr core, respectively.

The neutron radii with SLy4 and SkI4 interactions are almost identical when $A<122$. They increase rapidly when A beyond 122 with SkI4 interaction. Then we studied the neutron halos properties in hypernuclei with single-Λ and double-Λ in Zr isotopes using SkI4 interaction. The radii become small as the Λ numbers increase. The shrink effect in medium and heavy hypernuclei is not obvious as light ones. The neutron radii of single-Λ and double-Λ hypernuclei are almost identical with the even-N Zr isotopes. A neutron halo is predicted when neutron numbers is beyond 82. Because the last bound hypernucleus with double-Λ, $^{142}_{2\Lambda}$Zr, has two additional neutrons than ^{138}Zr, that will be helpful to form the giant neutron halo. Finally, we studied the Λ separation energies in our model with SkI4 interaction. We did not take the interaction between hyperons into consideration. The results are shown in Fig.4. For multi-Λ hypernuclei with ^{80}Zr and ^{138}Zr cores, the hyperon drip line hypernuclei are $^{100}_{20\Lambda}$Zr and $^{188}_{50\Lambda}$Zr, respectively.

4 Conclusion

We studied the properties of even-N Zr isotopes and their corresponding single-Λ and double-Λ hypernuclei are studied in the deformed Skyrme-Hartree-Fock approach. The prediction of neutron drip line depends on the Skyrme parameter used. The neutron drip line nucleus is ^{122}Zr with SLy4 interaction, and it will become ^{138}Zr if the interaction is replaced by SkI4. We compared the binding energy given by the two sets of parameters with the experimental data in Fig. 1. It is not possible to tell which Skyrme parameter is better for even-N Zr isotopes from the experimental data until now. The neutron halo structure is model dependent. The neutron drip line nuclei predicted with SkI4 and SLy4 interactions are ^{122}Zr and ^{138}Zr, and only the former force predict a neutron halo structure. The predicted hyperon drip line hypernuclei with the ^{80}Zr and ^{138}Zr cores are $^{100}_{20\Lambda}$Zr and $^{188}_{50\Lambda}$Zr, respectively.

References

1 Tanihata I, Hamagaki H, Hashimoto O et al. Phys. Rev. Lett., 1985, **55**: 2676—2679

2 Riisager K. Rev. Mod. Phys., 1994, **66**: 1105—1116

3 MENG J, RING P. Phys. Rev. Lett., 1996, **77**: 3963—3966

4 MENG J, RING P. Phys. Rev. Lett., 1998, **80**: 460—463

5 Grasso M, Yoshida S, Sndulescu N et al. Phys. Rev. C, 2006, **74**: 064317(7)

6 Vautherin D. Phys. Rev. C, 1973, **7**: 296—316

7 Blum V, Lauritsch G, Maruhn J A et al. J. Comput. Phys., 1992, **100**: 364—376

8 ZHOU X R, Schulze H J, Sagawa H et al. Phys. Rev. C, 2007, **76**: 034312(9)

9 Bender M, Rutz K, Reinhard P G et al. Phys. Rev. C, 1999, **60**: 034304

10 Tajima N, Bonche P, Flocard H et al. Nucl. Phys. A, 1993, **551**: 434—450